Real time spectroscopic ellipsometry on ultrathin (

Real time spectroscopic ellipsometry on ultrathin (<50 Å) hydrogenated amorphous silicon films on Si(100) and GaAs(100)

P. J. van den Oever, M. C. M. van de Sanden, and W. M. M. Kessels[a)]
Department of Applied Physics, Eindhoven University of Technology, P.O. Box 513, 5600 MB Eindhoven, The Netherlands

(Received 5 March 2007; accepted 14 May 2007; published online 28 June 2007)

Real time spectroscopic ellipsometry was used to determine the time evolution of the dielectric function, bulk thickness, and surface roughness during hot-wire chemical vapor deposition of hydrogenated amorphous silicon (*a*-Si:H). The amorphous silicon films were deposited on native-oxide-covered *c*-Si(100) and GaAs(100) substrates at temperatures in the range from 70 to 350 °C. Data analysis by a three layer optical model, consisting of substrate, bulk, and surface roughness layer, revealed that the dielectric function of the *a*-Si:H film changes in the initial growth regime ($d<50$ Å), which can be attributed to a higher optical band gap for films with a smaller thickness. It is argued that the origin of this higher band gap lies most likely in quantum confinement effects of the electron wave function in the ultrathin film, with possibly a small contribution of a higher hydrogen content in the ultrathin film. In addition, we show that the trends in surface roughness and bulk thickness are only marginally affected, regardless of whether the change in dielectric function with film thickness is incorporated in the data analysis. © *2007 American Institute of Physics*. [DOI: 10.1063/1.2749466]

I. INTRODUCTION

In recent years there has been a continuous trend towards the application of thinner films deposited on wafer substrates, which is primarily caused by the advancement of the semiconductor industry.[1] Ultrathin films of silicon are, for example, applied as interface passivation layer prior to the high-*k* dielectric deposition in metal-oxide-semiconductor capacitors fabricated from GaAs or Ge.[2–4] Another example can be found in the solar cell industry. Ultrathin films (thickness <50 Å) of hydrogenated amorphous silicon (*a*-Si:H) are applied as surface passivation layer, emitter of charge carriers, and back surface contact in silicon heterojunction (SHJ) solar cells.[5,6] For virtually all applications, the quality of the interface between the ultrathin film and the underlying substrate created in the first stages of growth is paramount.[7,8] Valuable information about the processes governing the interface formation can be extracted from the time evolution of film properties, such as surface roughness, bulk thickness, and dielectric function ε, in the early stages of deposition. For *a*-Si:H, for instance, the dielectric function reflects the main absorption in the film due to band-to-band transitions, while the evolution of the surface roughness yields information about nucleation processes and surface roughening or smoothening mechanisms.[9,10] Furthermore, it is believed that the hydrogen content in the *a*-Si:H film plays an important role in the initial stages of growth until a thickness of approximately 35 Å.[11,12] For such thin films, *in situ* and real time measurement of material properties requires very sensitive diagnostics, because of the limited thickness of the films and the dynamic nature of the initial growth regime.

Ultrathin *a*-Si:H films have been investigated both structurally and compositionally by a variety of techniques such as high-resolution transmission electron microscopy[8,13] and secondary ion mass spectrometry.[13,14] Although very powerful, these techniques are not applicable in real time measurements, are sample destructive, and do not provide fast process feedback. Alternatively, real time spectroscopic ellipsometry (RTSE) has demonstrated its sensitivity to subnanometer changes in thickness and can be applied in real time, providing instantaneous process feedback.[15,16] However, in most cases, the interpretation of the RTSE data is challenging as the analysis is based on a multilayer model that requires assumptions about the film structure and dielectric function of each consecutive layer. Within these assumptions, the RTSE data analysis gives the evolution of the bulk thickness and surface roughness during film growth, which also yields information about the initial stages of growth.[9,10,17]

The dielectric function of thick *a*-Si:H films can be determined directly from RTSE data by an elaborate procedure using a global regression analysis, when they are constant over a relatively large thickness range. This procedure determines the shape of the dielectric function and yields accurate results for the bulk thickness and surface roughness evolution. Nevertheless, parametrizations that assume a prescribed shape of the dielectric function are often preferred, because they are relatively uncomplicated, are defined in physically useful parameters, can be applied on a single, *ex situ* measurement, and allow for a controlled variation of the dielectric function. In contrast to thick films ($d\gg 50$ Å), many authors reported that the dielectric function of ultrathin *a*-Si:H films changes significantly with thickness.[18–23] However, in most RTSE analysis methods, such a change in dielectric function is not incorporated, although it might impact the

[a)]Author to whom correspondence should be addressed; electronic mail: w.m.m.kessels@tue.nl

information extracted about the first stages of *a*-Si:H growth.

Here we investigate the thickness dependence of the dielectric function and the evolution of the bulk and surface layer thicknesses in the first stages of growth by RTSE. The RTSE data analysis procedure for ultrathin *a*-Si:H films is improved compared to the well established procedure for thick films.[9,17] In Sec. II of this paper, we present the experimental arrangement, and in Sec. III, the RTSE data analysis is described in detail. The optical model is discussed and a method to extract the dielectric function directly from the ellipsometric data is presented. The commonly used Cody-Lorentz and Tauc-Lorentz parametrizations[24] are discussed and compared in Sec. III C on the basis of the fit quality for six RTSE data sets of *a*-Si:H growth under different conditions. Subsequently, we focus on the data analysis for ultrathin films and show that the quality of the fit can be drastically improved by allowing a controlled change in the dielectric function via a parametrization for films thinner than 50 Å. In Sec. IV C, we consider and discuss possible origins for the observed changes in dielectric function, such as a high hydrogen content in the interface layer or quantum confinement effects of the electron wave function. Finally, we discuss the impact of the improved RTSE data analysis on the deduced bulk thickness and roughness evolution in comparison with the analysis when using a thickness independent dielectric function for the initial stage of growth (Sec. IV D).

II. EXPERIMENTAL PROCEDURES

The *a*-Si:H films were deposited in an ultrahigh vacuum (UHV) setup consisting of two independently pumped stainless steel chambers separated by a central flange with the substrate mount. The setup features a low contaminant background, accurate substrate temperature control, and excellent optical access to the substrate for diagnostics such as spectroscopic ellipsometry (SE),[17] infrared absorption spectroscopy in the attenuated total reflection (ATR) geometry,[25] and second-harmonic generation.[26] More details on the experimental setup can be found in Ref. 17. Although SE and ATR were used simultaneously to monitor the deposition process of *a*-Si:H films by hot-wire chemical vapor deposition (HWCVD), we focus on the SE measurements in this study.

Due to a possible substrate material dependency, both Si(100) and GaAs(100) substrates (50×20 mm^2) with surface native oxide were used. In addition, GaAs substrates have a high infrared transmission at elevated substrate temperatures, which was required for the ATR measurements. The substrates were cleaned ultrasonically in ethanol for 20 min and subsequently blown dry with nitrogen. The GaAs substrates could be reused by removing the silicon remnants from previous depositions by a wet chemical etch in a 0.1 M/1 KOH solution for ~30 min prior to the cleaning procedure. After mounting the substrate and pumping down, the setup and the substrate were heated to 70 and 150 °C, respectively, and left over night to reach a base pressure below 2×10^{-8} mbar.

Before the actual deposition by HWCVD in undiluted SiH_4, the substrate was cooled down or heated to the desired temperature. A SiH_4 flow of 3 SCCM (cubic centimeter per minute at STP) (Praxair, purity >99.995% and with additional purification) resulted in a deposition pressure of $\sim8\times10^{-3}$ mbar. The SiH_4 was decomposed by a coiled tungsten filament (0.4 mm diameter), which was located approximately 11 cm from the substrate. This filament was resistively heated to a temperature of ~2000±200 °C by a dc current of 9.5 A. Before deposition, the substrate was protected from direct exposure to generated radical species by an automated shutter located directly in front of the substrate. The used pressure and filament-substrate distance correspond to optimal conditions for hot-wire *a*-Si:H deposition as reported by Kessels *et al.*[17] and Molenbroek *et al.*[27] In the present study, films were deposited on GaAs at substrate temperatures of 70, 150, 250, and 350 °C, while for the depositions on *c*-Si, only temperatures of 150 and 250 °C were used. The substrate temperature was controlled using a previously established relation between the actual substrate temperature and the temperature of the central flange measured by a thermocouple. The reported substrate temperatures are in good agreement with the temperatures extracted from the RTSE measurements using the temperature dependence of the substrate dielectric function. For all these conditions, the deposition rate was approximately 30 Å/min. Table I summarizes the most important deposition conditions for the six samples discussed in this paper, as well as the band gap determined by the Tauc procedure,[28] the refractive index at 2 eV, and the atomic hydrogen content determined by ATR infrared absorption spectroscopy. Although the study is focused on ultrathin films ($d<50$ Å), the depositions were continued to a film thickness of ~1500 Å to accurately determine the bulk material properties.

The spectroscopic ellipsometry measurements were carried out using a rotating compensator spectroscopic ellipsometer (J.A. Woollam M-2000U), collecting 476 wavelengths in a spectral range from 1.24 to 5.0 eV. The ellipsometry light beam entered and exited the vacuum chamber via strain-free windows (Bomco Inc.) and the angle of incidence was approximately 59°. RTSE measurements were taken in real time before, during, and after the film deposition. Averaging 25 spectra, the time resolution of the RTSE measurements was ~3.5 s, giving an excellent signal-to-noise ratio.

III. RTSE DATA ANALYSIS

A. General information

In this section, we introduce the data analysis procedures needed to extract useful information from the SE measurements. Spectroscopic ellipsometry measures the change in polarization state of light upon reflection off a sample in terms of the ellipsometric angles Ψ and Δ, which can also be expressed in the *pseudodielectric* function of the sample ($\langle\varepsilon\rangle=\langle\varepsilon_1\rangle+i\langle\varepsilon_2\rangle$). To extract physical quantities of interest such as the dielectric function, bulk thickness, and surface roughness from the pseudodielectric function, a multilayer optical model is needed. Throughout this paper we use a relatively simple three layer optical model, consisting of sub-

TABLE I. An overview of the *a*-Si:H samples used in this study. The Cody-Lorentz parameters, Tauc band gap (E_{Tauc}), and refractive index at 2 eV ($n_{2\mathrm{eV}}$) determined by SE are given for *a*-Si:H grown on *c*-Si and GaAs substrates with native oxide at deposition temperatures of 70, 150, 250, and 350 °C. The reported atomic hydrogen content [H] was determined from the ATR infrared spectroscopy measurements. Also the MSE between fit and data, averaged over all consecutive time slices, is given for Cody-Lorentz and Tauc-Lorentz parametrizations of the dielectric function. In the first data column, the typical errors in the parameters are presented.

Sample number	1	2	3	4	5	6
Substrate material	Si(100)	Si(100)	GaAs(100)	GaAs(100)	GaAs(100)	GaAs(100)
T_{sub} (°C)	150±15	250	70	150	250	350
E_{Tauc} (eV)	1.75±0.03	1.72	1.81	1.81	1.72	1.64
$n_{2\mathrm{eV}}$	4.22±0.02	4.45	3.78	4.14	4.43	4.61
[H] (at. %)	17±4[a]	[b]	25[a]	23[a]	18[a]	14[a]
E_{inf}	1.39±0.05	1.02	1.43	1.39	1.32	1.29
A	79±2	92	85	81	77	77
Γ	2.40±0.01	2.43	2.56	2.37	2.32	2.35
E_0 (eV)	3.74±0.01	3.69	3.75	3.75	3.67	3.62
E_g (eV)	1.59±0.02	1.52	1.63	1.67	1.55	1.43
E_p (eV)	1.17±0.05	1.33	1.70	1.25	1.02	0.98
Ave. MSE CL	3.28	1.74	2.24	1.44	2.64	2.25
Ave. MSE TL	3.78	2.91	3.19	2.91	3.74	4.17

[a]The complexity of the data analysis for the ATR geometry leads to a higher experimental error for the atomic hydrogen content [H] and most likely to a systematic error, yielding a slightly higher atomic hydrogen content than normal incidence transmission infrared measurements.
[b]Could not be determined due to insufficient transmission of infrared light through the Si(100) substrate at a temperature of 250 °C.

strate, film, and surface roughness layer, for the RTSE data analysis. The dielectric function ($\varepsilon=\varepsilon_1+i\varepsilon_2$) of the substrate can easily be extracted from the measurements before deposition, but the extraction of the dielectric function of the film from the RTSE data after deposition is more complex. The film's dielectric function can be determined directly without assumptions about its spectral shape by a global regression analysis (method 1), or it can be determined indirectly by using a parametrization that prescribes a specific shape of the dielectric function versus photon energy (method 2). Method 2 is often preferred as it is relatively uncomplicated, provides direct access to physically useful parameters, and can be applied to a single *ex situ* measurement at the final thickness, which is not the case for method 1. Section III B discusses both methods to determine the dielectric function in detail. After the dielectric function of the film has been determined (either method 1 or 2), the bulk thickness and surface roughness layer thickness can be extracted from the RTSE data. At all points in time, a realistic optical model should provide an accurate description of the measured Ψ and Δ values while maintaining the lowest level of complexity (number of fitting parameters) possible.

In our case, all RTSE data were analyzed with the EASE 2.30 software package provided by J.A. Woollam Co., Inc.[29] using the three layer model with bulk film thickness (d_b) and surface roughness layer thickness (d_s) as free parameters. The total film thickness is defined as $d_t=d_b+(1-f_v)d_s$, in which f_v is the void fraction in the surface roughness layer (see Sec. III B). The model was fitted to each spectrum, minimizing the mean square error (MSE) between fit and data. The MSE is defined as

$$\mathrm{MSE}=\sqrt{\frac{1}{2N-M}\sum_{i=1}^{N}\left[(\langle\varepsilon_1\rangle_i^{\mathrm{exp}}-\langle\varepsilon_1\rangle_i^{\mathrm{mod}})^2+(\langle\varepsilon_2\rangle_i^{\mathrm{exp}}-\langle\varepsilon_2\rangle_i^{\mathrm{mod}})^2\right]}. \quad (1)$$

In this expression, N is the number of measured wavelengths, M the number of fit variables in the model, and $\langle\varepsilon_1\rangle_i^{\mathrm{exp}}$, $\langle\varepsilon_1\rangle_i^{\mathrm{mod}}$, $\langle\varepsilon_2\rangle_i^{\mathrm{exp}}$, and $\langle\varepsilon_2\rangle_i^{\mathrm{mod}}$ are the real and imaginary parts of the experimental or modeled pseudodielectric functions at wavelength i calculated directly from the experimental or modeled ellipsometric angles Ψ and Δ. In the fit procedure, the final fit parameters at one point in time provide the starting values for fitting the next time point.

B. The optical model

1. Substrate dielectric function

The substrate dielectric function used in the model was extracted from the RTSE measurements before deposition by direct numerical inversion[30] and is in good agreement with the tabulated values for GaAs(100) or Si(100) plus native oxide. The use of this so-called "pseudosubstrate" method is justified by the relatively small native oxide thickness

(~20 Å) compared to the probing wavelength (>2450 Å), which precludes interference effects in these layers. Furthermore, we assume no substrate modification during deposition, which is a reasonable assumption because of the remote nature of the HWCVD technique used in this study.

2. Film dielectric function

The dielectric function of the *a*-Si:H film was determined directly from the RTSE data in a procedure based on the three layer substrate-film-roughness model by a global regression analysis using at least six RTSE spectra, equally distributed in time over the part of the deposition in which the material properties can be assumed constant (i.e., excluding the initial regime of film growth, $d \gg 50$ Å). This procedure (method 1) determines the dielectric function in a Kramers-Kronig consistent way without *ab initio* assumptions about the shape of the dielectric function (i.e., no parametrization), the bulk thickness, and the surface roughness layer thickness. It minimizes the MSE by fitting the shape of the dielectric function, the bulk thickness, and surface roughness layer thickness for all selected time slices simultaneously. In this procedure, the surface roughness is represented by a Bruggeman effective medium approach, which will be discussed below. This relatively fast analysis, which uses tabulated values for the *a*-Si:H dielectric function as an initial guess, yields a dielectric function that corresponds to the minimum in the MSE and is in good agreement with results obtained by the more elaborate global dynamic minimization scheme described by An *et al.*[31] The dielectric function resulting from the above mentioned procedure can be used directly to extract the bulk thickness and the surface roughness layer thickness from the RTSE data.

In some cases, a parametrization of the dielectric function (i.e., method 2) is preferable as discussed previously. Suitable parametrizations for the *a*-Si:H dielectric function are the Kramers-Kronig consistent Tauc-Lorentz (TL) or Cody-Lorentz (CL) model, which are both based on the assumption of parabolic bands but either with a constant momentum matrix element (TL) or a constant dipole matrix element (CL).[24] For both parametrizations, the imaginary part of the dielectric function can be written as[32]

$$\varepsilon_2(E) = \begin{cases} 0, & 0 < E \leq E_g \\ G(E)\dfrac{AE_0\Gamma E}{[(E^2 - E_0^2)^2 + \Gamma^2 E^2]}, & E > E_g, \end{cases} \tag{2}$$

with A the amplitude, E_0 the peak transition energy, Γ the broadening term, and E_g the band gap energy. $G(E)$ defines the near band gap behavior, which is different for, respectively, the TL (G_{TL}) and CL (G_{CL}) models:

$$G_{\mathrm{TL}}(E) = \frac{(E - E_g)^2}{E^2}, \tag{3}$$

$$G_{\mathrm{CL}}(E) = \frac{(E - E_g)^2}{(E - E_g)^2 + E_p^2}. \tag{4}$$

In the CL expression, E_p is a transition energy that separates the Cody shaped absorption onset from the Lorentzian behavior. The real part of the dielectric function $\varepsilon_1(E)$ is, in both cases, obtained by Kramers-Kronig integration of $\varepsilon_2(E)$, given by

$$\varepsilon_1(E) = \varepsilon_1(\infty) + \frac{2}{\pi} P \int_{E_g}^{\infty} \frac{\xi \varepsilon_2(\xi)}{\xi^2 - E^2} d\xi, \tag{5}$$

where $\varepsilon_1(\infty)$ is a fitting constant that allows $\varepsilon_1(E)$ to converge to values different from unity, and P stands for the Cauchy principal part of the integral.

In previous studies, we also used the Tauc-Lorentz parametrization directly (method 2) to determine the dielectric function of hot-wire deposited *a*-Si:H,[17] which is justified when the parametrization is a good representation of the film's dielectric function. However, when this is not the case or when the dielectric function of the deposited film is unknown, a parametrization cannot be used and the dielectric function needs to be determined directly from the RTSE data (for example, using method 1). This dielectric function obtained can subsequently be used to fit the consecutive RTSE spectra in time as well as to develop an adequate parametrization for the dielectric function of the deposited film. In the next section, we will determine which parametrization is best suited to describe the dielectric function of *a*-Si:H deposited at various substrate temperatures on Si(100) and GaAs(100) substrates covered with native oxide.

3. Surface roughness

The dielectric function of the surface roughness layer (ε_s) was modeled using a Bruggeman effective medium approximation, which is assumed to consist of voids with a fraction f_v and of the underlying film with a fraction $f_f = 1 - f_v$:

$$0 = (1 - f_v)\frac{\varepsilon_f - \varepsilon_s}{(\varepsilon_f + 2\varepsilon_s)} + f_v \frac{\varepsilon_v - \varepsilon_s}{(\varepsilon_v + 2\varepsilon_s)}. \tag{6}$$

In this expression, ε_f and ε_v represent the dielectric function of the film and voids ($\varepsilon_1 = 1$ and $\varepsilon_2 = 0$ for all photon energies), respectively. The Bruggeman effective medium approximation is commonly used to model the surface roughness layer in ellipsometry data analysis, and its validity was evaluated[33] in detail by Fujiwara *et al.* They found that a void fraction f_v of 0.5 gives an excellent representation of the surface roughness layer for bulk *a*-Si:H growth. In a similar analysis carried out on our RTSE data, we came to the same conclusion. Therefore, we use a void fraction of 0.5 in the Bruggeman effective medium approximation of the surface roughness layer in this study.

C. The choice between Tauc-Lorentz or Cody-Lorentz parametrization

In this section, we evaluate which parametrization is best suited to describe the dielectric function of *a*-Si:H using actual RTSE data from depositions. Figure 1 shows the dielectric function of the *a*-Si:H film deposited at 150 °C on a GaAs substrate determined directly from the RTSE data using method 1 as described above. Furthermore, the figure shows the best fits to this dielectric function using the CL and TL parametrizations. As can be seen from the residue values between data and fit depicted in the lower part of Fig.

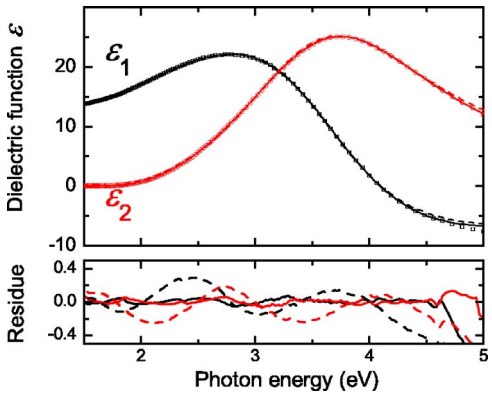

FIG. 1. (Color online) The real and imaginary parts of the dielectric function (ε_1 and ε_2) of an a-Si:H film deposited at 150 °C on a GaAs substrate determined by a global regression analysis using 12 time slices of RTSE data. The parametrizations of the dielectric function using the Tauc-Lorentz (dashed line) and Cody-Lorentz (solid line) models are also shown, as well as the corresponding residue values.

1, the fit using the CL parametrization is significantly better. Only for photon energies above 4.5 eV, a small deviation between parametrization and the directly determined dielectric function is observed. For the depositions at other substrate temperatures and types, we also found that the CL parametrization was better than the TL parametrization.

Table I shows the CL parameters $\varepsilon_1(\infty)$, A, E_0, Γ, E_g, and E_p extracted from the fits for the six a-Si:H depositions considered in this study. These CL as well as the TL parametrizations determined by fitting the directly extracted dielectric function were subsequently used to extract the time evolution of the bulk thickness and surface roughness layer thickness from the consecutive RTSE spectra. The time-averaged MSE values associated with these fits are also given in Table I. Comparing the averaged MSE obtained using the CL and the TL parametrizations confirms the conclusion that the CL model is a better representation of the a-Si:H dielectric function for films deposited on both c-Si and GaAs substrates at evaluated temperatures. The superiority of the CL over the TL parametrization is supported by various other studies,[24,34] and therefore, in all subsequent analysis, the Cody-Lorentz parametrization will be used.

IV. RTSE DATA ANALYSIS FOR ULTRATHIN FILMS

A. RTSE data analysis with a thickness independent dielectric function

The use of a thickness independent dielectric function of the bulk layer has become a standard procedure in analyzing RTSE data of thin film deposition processes.[9,17] Here we apply the data analysis procedure described in the previous section under the assumption of a thickness independent dielectric function to our data and focus on the early stages of growth. The bulk dielectric function was extracted directly from the RTSE data (method 1) and subsequently parametrized by the Cody-Lorentz model, which was used to fit the consecutive RTSE spectra for bulk thickness and surface roughness. Figure 2 shows the fit results using the three layer model (as described in Sec. III) in the first 180 s of a-Si:H deposition on GaAs substrates at various temperatures. For

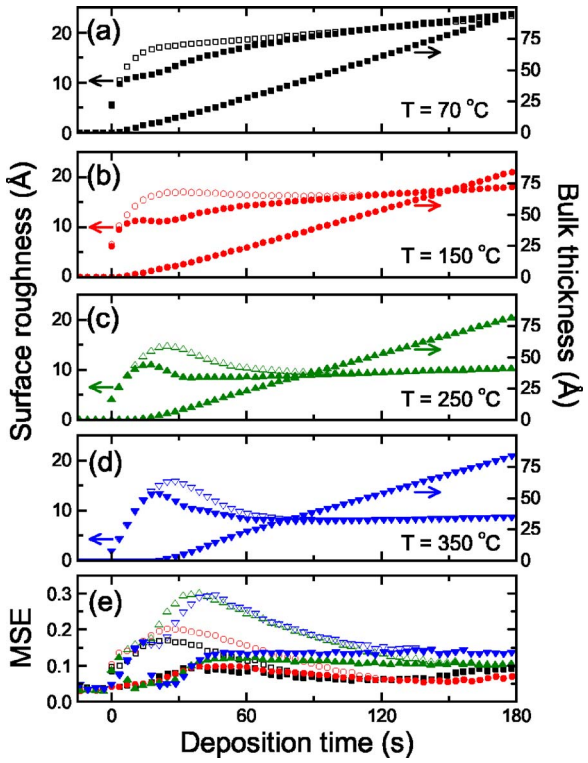

FIG. 2. (Color online) The surface roughness (left axis) and bulk thickness (right axis) evolution in the first 180 s of the deposition extracted from the RTSE data using the analysis with fixed (open symbols) and variable band gaps (solid symbols) for films deposited on GaAs substrates at substrate temperatures of (a) 70 °C, (b) 150 °C, (c) 250 °C, and (d) 350 °C. The bulk thickness is the same for both analysis methods. (e) The mean square error (MSE) associated with the fits. In (e) the symbol types correspond to those in (a)–(d).

brevity, we only show the temperature series on GaAs substrates in this section, but the depositions on c-Si show a similar behavior with slightly lower absolute values of the surface roughness. As expected, the bulk layer thickness increases linearly as a function of the deposition time for all substrate temperatures and the total film thickness after 180 s deposition is approximately 90 Å for all films. In the first 20 s of the deposition, the surface roughness d_s increases very fast for all temperatures to a level of approximately 15 Å as can be seen in Figs. 2(a)–2(d). Thereafter, the surface roughness evolution behaves differently for the various temperatures. For the deposition at 70 °C, the roughness increases monotonically to ~24 Å, while the depositions at 150, 250, and 350 °C show a substrate temperature dependent decrease that is followed by a gradual increase to values of ~18, ~10, and ~9 Å after 180 s of deposition, respectively. After 180 s, the surface roughness increases slowly for all temperatures (not shown), which is typical for steady state a-Si:H growth. It is clear from the results in Fig. 2 that the surface roughness for thick films decreases with increasing substrate temperature. A slightly different behavior of the bulk thickness and surface roughness versus deposition time was reported previously by our group for a-Si:H deposited on crystalline silicon covered with native oxide.[17] The MSE depicted by the open symbols in Fig. 2(e), which is a measure for the quality of the fit (see Sec. III A), reaches a maximum at 30–60 s deposition time. In the next 60–90 s, it

decreases significantly, after which it remains approximately constant. Fujiwara *et al.* found a similar maximum in fit error for plasma enhanced chemical vapor deposited *a*-Si:H films, which was attributed to a change in the dielectric function of the ultrathin film combined with an increase in the void fraction of the Bruggeman effective medium approximation used to describe the surface roughness.[33] In the next section, it will be shown that the MSE does not show a clear maximum when the dielectric function comprises a thickness dependent band gap.

B. RTSE data analysis with variable band gap

The broad peak in fit error (MSE) observed in Fig. 2(e) coincides with the region in which most of the dynamics in the surface roughness evolution occurs. This questions the reliability of the suggested data analysis procedure in this region. To improve the fit quality in this region, few options were evaluated. One possibility is that the first atomic layers that form in a deposition process adopt the chemistry of the substrate plus overlayer (GaAs oxide for GaAs and SiO_2 for Si). In this case, a thin interface layer consisting of Si–O bonds might be formed. Alternatively, when there is any surface roughness on the starting substrate, the first atomic layers will be an effective medium of substrate-overlayer and film. Therefore, various interface layers with a typical thickness of 10–25 Å, consisting of SiO_2, an effective medium approximation (EMA) of SiO_2 and *a*-Si:H, and an EMA of GaAs oxide and *a*-Si:H, have been implemented in the fitting procedure in an attempt to improve the fit in the initial part of the deposition. For all these attempts, the interface layer thickness was reduced to zero after approximately 50 Å of deposition, which does not correspond to the physical mechanisms of Si–O bond formation on the interface or the formation of an intermix layer of substrate-overlayer and *a*-Si:H film. In another attempt to improve the fit in the initial part of the deposition, the band gap in the CL parametrization of the *a*-Si:H was allowed to vary. The choice for a varying *a*-Si:H band gap was inspired by other studies that reported a higher band gap for ultrathin films, such as the studies of *a*-Si:H/SiO_2 multilayer structures by Lockwood and co-workers[21,22] and a typical dielectric function of ultrathin *a*-Si:H observed by RTSE.[33] As can be seen in Fig. 2(e), incorporating a varying band gap lowers the MSE values in the first 120 s of the deposition significantly compared to the analysis with a thickness independent dielectric function that was described in the previous section. The surface roughness evolution is marginally affected by the inclusion of variable band gap in the data analysis procedure as is shown in Figs. 2(a)–2(d) and discussed in Sec. IV D. Figure 3(a) shows the band gap variation as a function of the total film thickness deduced from the RTSE analysis for all depositions. The behavior of the band gap energy as a function of the film thickness shows similar behavior for all films studied, regardless of the deposition temperature or substrate used. In the first 50 Å of the deposition, the band gap decreases from ~3 eV to the bulk band gap value, which varies between 1.5 and 1.7 eV depending on the substrate temperature.[35] The depositions on *c*-Si show the same trend, but due to the limited optical contrast between the *c*-Si substrate and the depositing film, it was not possible to determine the band gap in the first 15 Å of growth. As an example, the corresponding change in the imaginary part of the dielectric function ε_2 [from Eqs. (2) and (4)] is shown in Fig. 3(b) for a total film thickness d_t that progresses from ultrathin films to bulk values (≥50 Å). Besides the increase of the band gap energy, also the height of ε_2 decreases for ultrathin films.[36] A similar reduction of the height of the dielectric function was predicted by atomistic calculations for Si quantum dots by Wang and Zunger.[37]

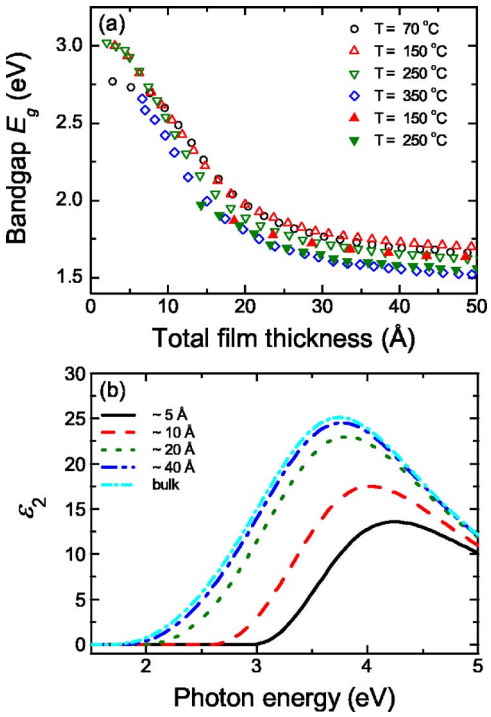

FIG. 3. (Color online) (a) The variation of the band gap parameter E_g as a function of the film thickness deduced from the fits of the RTSE spectra. Open symbols correspond to films deposited on GaAs substrates and closed symbols to films deposited on *c*-Si. (b) An example of the imaginary part of the dielectric function ε_2 of an *a*-Si:H film deposited at 150 °C on a GaAs substrate in the thickness range from ~5 Å to ≥50 Å (bulk film).

Furthermore, it has been verified that a varying void fraction in the surface roughness layer (affecting the amplitude of the dielectric function, not the band gap) only yields a marginal reduction of the MSE (not shown). Therefore, we have chosen to neglect a possible change in void fraction in our analysis to avoid increased complexity of the optical modeling. In Sec. IV D, the consequences of including a variable band gap on the surface roughness evolution extracted from the RTSE modeling will be examined, but, first, possible origins of the thickness dependence of the band gap will be discussed.

C. Thickness dependent band gap: Physical origin

Several authors have observed a higher band gap for ultrathin *a*-Si:H films compared to the bulk value using various diagnostics. Yet the discussion about the origin of this effect has not completely settled.[18–23] In the literature, two explanations for the increased band gap of ultrathin films are

commonly suggested: (i) an increased hydrogen content and (ii) quantum confinement effects of the electron wave function. Fujiwara *et al.* attributed the observed ~0.2 eV blueshift compared to the bulk dielectric function of a 17 Å thick *a*-Si:H film deposited on a *c*-Si substrate to a higher H content in the initial layer.[33] In an earlier study, the same group reported a blueshift of the band gap for *a*-Si:H as well as for *c*-Si films with decreasing film thickness. For the *c*-Si films, this effect was attributed to confinement of the electron wave function in the material, while for the *a*-Si:H films, an excess H content was suggested as the cause for the band gap shift.[18]

Recently, we demonstrated that *a*-Si:H films deposited on GaAs substrates also have a hydrogen rich interface layer,[11] while it is generally accepted that the band gap E_g increases with hydrogen content [H] for bulk *a*-Si:H.[38,39] Therefore, excess hydrogen content is a likely candidate to contribute to the increased band gap for ultrathin films. Quantum confinement, on the other hand, can take place when the film thickness is smaller than the localization length of the electron wave function. A well known example can be found in the etching of *c*-Si to a porous material. When the film becomes more porous, an increase in band gap is observed by a clear blueshift of the photoluminescence (PL) peak energy.[40,41] For *a*-Si:H, however, conflicting results have been reported in the literature. In the etching of *a*-Si:H to a porous variant, the PL peak energy remained at the same position,[42] which indicates that the localization length of the electron wave function might be too short for quantum confinement effects on the length scales in the porous amorphous silicon (30–50 Å). This was also suggested by Mott, who estimated the localization length of the electron wave function in *a*-Si:H to be ~10 Å compared to ~50 Å in *c*-Si.[43] On the basis of this statement, quantum confinement effects in *a*-Si:H films thicker than ~10 Å are unlikely. Nevertheless, Park *et al.* have shown that quantum confinement is possible in 24 Å sized *a*-Si:H quantum dots in an *a*-SiN_x:H matrix.[44] This observation is supported by theoretical work by Nishio *et al.*, who calculated the size dependence of the peak energy in the emission of *a*-Si quantum dots in an *a*-SiN_x:H matrix[45] and found perfect agreement with the experimental results of Park *et al.* More experimental evidence for quantum confinement in 10–30 Å thick hydrogen deficient *a*-Si layers was given by Lockwood and co-workers, who measured the blueshift of the photoluminescence peak energy in molecular beam epitaxy (MBE) grown *a*-Si/SiO_x superlattices as a function of the *a*-Si film thickness. The blueshift observed was corroborated by independent soft x-ray Si $L_{2,3}$ edge absorption spectroscopy, which probes the shift in the conduction band minimum and valence band maximum.[21,22] The observed energy gap shift $E_g - E_{g,\mathrm{bulk}}$ could be accurately fitted by an effective mass model for one dimensionally confined Si assuming infinite potential barriers:

$$E_g - E_{g,\mathrm{bulk}} = \frac{C}{d^2}, \tag{7}$$

with the confinement parameter C defined as

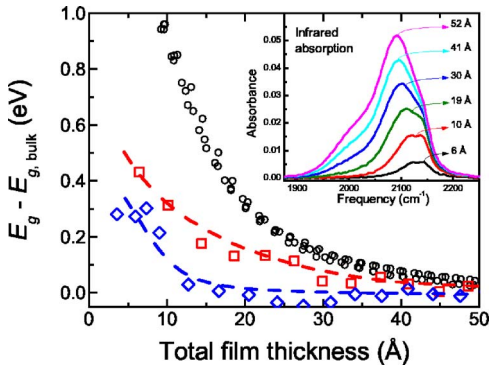

FIG. 4. (Color online) The band gap shift $E-E_g$ calculated on the basis of the hydrogen content deduced from *in situ* infrared absorption measurements shown for the depositions at substrate temperatures of 70 °C (open squares) and 350 °C (open diamonds). The lines serve as a guide for the eyes. Furthermore, the band gap shifts deduced from the RTSE analysis are represented by the open circles for all substrate types and temperatures used. The inset shows the absorption spectra of the film deposited at 70 °C at several values of the film thickness. These absorption spectra were used to calculate the band gap shift on the basis of the hydrogen content.

$$C = \frac{\pi^2\hbar^2}{2}\left(\frac{1}{m_e^*} + \frac{1}{m_h^*}\right). \tag{8}$$

In this expression, m_e^* and m_h^* are the electron and hole effective masses and d is the film thickness. The experimental results by Lockwood and co-workers were reproduced theoretically by Nishida, who calculated the electronic structures of ultrathin Si(100) films and concluded that the MBE grown *a*-Si are almost crystalline.[46] More theoretical support for the existence of the quantum confinement effect come from Allan *et al.*, who calculated the electronic structure of amorphous silicon clusters within the tight binding approximation and concluded that one should expect blueshifts with the reduction in size comparable to what is reported for *c*-Si clusters.[47] In a separate publication, they reported that quantum confinement effects can be expected in *a*-Si layers with a thickness below 30 Å.[48] In the next two sections, we will discuss an increased hydrogen content as well as the quantum confinement effect as possible explanations for the higher band gap for ultrathin films with respect to the band gap value for bulk films.

1. Increased hydrogen content

Several studies have shown that the initial layer in *a*-Si:H growth is relatively hydrogen rich compared to the bulk film.[11,12] The contribution of this higher hydrogen content near the interface to the increase of the band gap observed can be estimated by a measurement of the hydrogen content as a function of the film thickness. As mentioned in Sec. II, the hydrogen content was measured *in situ* and in real time by infrared absorption spectroscopy in the so-called ATR geometry[11,12,15] simultaneously with the RTSE experiments. The inset in Fig. 4 shows the infrared absorption due to SiH and SiH_2 groups in an *a*-Si:H film with increasing thickness deposited at 70 °C. Assuming thickness independent absorption cross sections of the SiH and SiH_2 groups,[49] the infrared absorption spectra were used to determine an upper estimate of the bonded atomic H content as a function

of the film thickness. As reported in Ref. 11, this analysis revealed a hydrogen rich interface layer, which was corroborated by secondary ion mass spectrometry measurements. Subsequently, the value of the band gap corresponding to the hydrogen content at a certain film thickness was calculated from the relation between the hydrogen content [H] and band gap derived from measurements for thick *a*-Si:H films: $E_g = (1.34 \pm 0.06) + (21 \pm 4) \times 10^{-3}$ [H]. This relation is in good agreement with results presented in Refs. 50–52. Figure 4 shows the band gap shift $E_g - E_{g,\mathrm{bulk}}$ with respect to the bulk value $E_{g,\mathrm{bulk}}$ calculated from the H content as a function of the total film thickness as well as the band gap shifts obtained from the RTSE measurements. Both data sets show a higher band gap shift for thinner films, but the band gap shifts obtained from the RTSE measurements are clearly higher than the ones deduced from the H content measured by infrared absorption spectroscopy. These observations suggest that the observed band gap shift cannot be fully attributed to the increased hydrogen content. Moreover, the band gap shifts extracted from the RTSE measurements are independent of the substrate temperature, while the band gap shifts deduced from the infrared measurements are not. This indicates that the observed higher band gap for thinner films is probably not completely caused by the increased hydrogen content of the ultrathin films.

Another argument supporting the conclusion that the higher band gap for ultrathin films is not caused by a high initial hydrogen content follows from RTSE modeling of thick *a*-Si:H films. When we assume that a hydrogen rich interface layer is responsible for the increased band gap, the optical model used for the RTSE data analysis of films thicker than ~50 Å should be extended with a high band gap interface layer between substrate and bulk *a*-Si:H film. The inclusion of such a high band gap interface layer in the optical model, however, does not result in lower but in higher MSE values for the fits of the RTSE spectra of the thick films. The quantum confinement effect, on the other hand, is only present for ultrathin films and disappears for films thicker than ~50 Å, which is exactly what we observed in our data. In addition, it was shown by Jun *et al.* that the blueshift in the dielectric function for thin *a*-Si:H films remains after all atomic H was removed from the samples by annealing the *a*-Si:H at 600 °C.[20] The above mentioned observations basically exclude hydrogen as the only origin of the increased band gap observed for ultrathin films. However, a minor contribution of the excess hydrogen content to the higher band gap for ultrathin films cannot be excluded on the basis of these data.

2. Quantum confinement

As discussed before, an alternative explanation for the increased band gap observed in the experiments is the quantum confinement effect. Figure 5 shows the band gap shift $E - E_g$ deduced from the RTSE measurements and several literature values of band gap shifts that have been attributed to quantum confinement effects in *a*-Si:H, such as the studies reported by Lockwood *et al.*,[22] Allan *et al.*,[48] and Nishida.[46] The lines in Fig. 5 are fits by the simple approximation of one-dimensional (1D) quantum confinement given

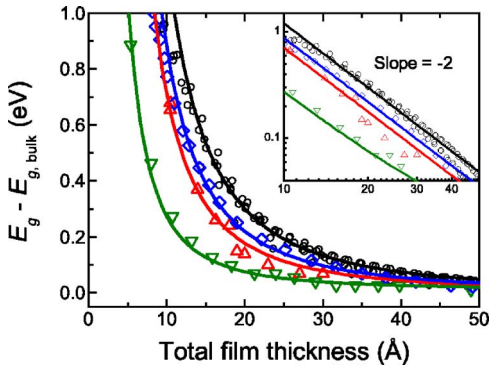

FIG. 5. (Color online) The band gap shift $E - E_g$ as a function of the total film thickness deduced from the RTSE analysis (open circles). Also values from thin film structures that include amorphous silicon reported in the literature are shown (triangle up, Ref. 21; triangle down, Ref. 48; and diamonds, Ref. 46). The lines are fits to the data using a $1/d^2$ relation that is characteristic of 1D quantum confinement. The inset shows the same data with double logarithmic axes.

by Eq. (7), while the inset shows the same data on a double logarithmic scale. The band gap shift determined by the RTSE measurements shows a $1/d^2$ behavior that is characteristic of quantum confinement. Only for a film thickness $< \sim 10$ Å do the data and the fit show a deviation, which could be caused by the limited optical contrast between substrate and film in the RTSE measurements for such thin films. This deviation might also be caused by scattering effects from interfaces and surfaces, creating broadening effects that make detection of quantum confinement effects more difficult. For films thicker than ~10 Å, however, the lateral variation in the roughness of interfaces and surfaces on the length scale needed for quantum confinement (~50 Å) is relatively small (~1–2 Å) compared to the film thickness. Therefore, only a slight broadening of the transitions due to roughness of interfaces and surfaces is expected, which will not prevent quantum confinement effects from being detected.

The extracted value for the confinement parameter C of 120 ± 4 eV Å^2 is in fair agreement with literature values for the electron and hole effective masses in *a*-Si:H. Using $m_e^* = 0.3 \pm 0.1$ and $m_h^* = 1.0 \pm 0.1$ for the effective masses of electrons and holes in *a*-Si:H,[53] respectively, a confinement parameter of 165 ± 70 eV Å^2 is found.[54] These results clearly suggest quantum confinement as the origin of the higher band gap for ultrathin films.

D. Implications of the surface roughness evolution

For the RTSE fitting in this study, we chose to adapt a varying band gap in the first 50 Å of film growth to account for the change in the dielectric function. As was demonstrated in Fig. 2(e), this modification to the data analysis procedure significantly improves the fit quality and produces consistent fit results. In Figs. 2(a)–2(d), we compare the behavior of the surface roughness as a function of the deposition time obtained from the RTSE analysis using the thickness independent band gap (Sec. IV A) and the varying band gap method (Sec. IV B). When the varying band gap method is used for fitting, the initial increase in surface roughness is

smaller compared to the method with the thickness independent band gap. The surface roughness is also lower in the subsequent region until approximately 90 s deposition time, when the band gap is varied. For films thicker than 50 Å (~90 s deposition time), no difference between both analysis methods is observed. The general trends as described in Sec. IV A, however, are the same for both fitting methods. For the temperature range studied, these trends in the surface roughness versus deposition time have been attributed to physical phenomena in previous work: (a) heterogeneous nucleation in the first 20 s of growth (typical film thickness 10 Å), followed by (b) coalescence of the nuclei and temperature dependent smoothening on a relatively small lateral length scale (film thickness from 10 to ~75 Å), and finally, (c) surface roughening on larger lateral length scales (films thicker than ~75 Å).[9,10,17] The relatively minor changes in the observed trends imply that the conclusions based on the surface roughness evolution drawn by several authors remain valid. For instance, the nucleation, density on the native oxide surface calculated from the initial roughness increase due to heterogeneous nucleation would be in the range of $(1-2)\times 10^{13}$ cm^{-2} for both fitting methods.

V. CONCLUSIONS

The thickness evolution of the dielectric function of *a*-Si:H was studied by real time spectroscopic ellipsometry during hot-wire chemical vapor deposition. The dielectric functions of thick *a*-Si:H films were determined directly from the data without assumptions about their shape and could be parametrized best by the Cody-Lorentz rather than by the Tauc-Lorentz parametrization. For ultrathin films ($d<50$ Å), the data analysis procedure using a constant dielectric function over the whole film thickness could be improved significantly by incorporating a higher band gap for thinner films via the Cody-Lorentz parametrization. Although the varying band gap in the RTSE analysis greatly improved the fit quality in the first 50 Å, the evolution of the surface roughness was only marginally affected. The magnitude of the surface roughness decreases slightly in the first 50 Å of growth, but the general trends with film thickness described in previous studies remain nearly unaffected. This implies that spectroscopic ellipsometry can be used with confidence for the analysis of the surface roughness of ultrathin films.

Two possible explanations for the higher band gap of ultrathin films that were suggested in the literature have been discussed in this paper. First, we argued that the higher hydrogen content in the interface region measured by infrared absorption spectroscopy cannot explain the higher band gap for ultrathin films. Alternatively, we demonstrated that this band gap shift can be accurately fitted by a $1/d^2$ relation, which is characteristic of 1D quantum confinement. Furthermore, our data, show resemblance with studies (both experimental as well as modeling studies) that attribute the higher band gap in ultrathin *a*-Si:H structures to quantum confinement effects. On the basis of our data, we suggest therefore that the observed phenomenon of a higher band gap for ultrathin films is caused by quantum confinement.

ACKNOWLEDGMENTS

M. J. F. van de Sande, J. F. C. Jansen, and J. J. A. Zeebregts are acknowledged for their skillful technical assistance. Dr. R. W. Collins (University of Toledo) is thanked for proofreading the manuscript and constructive comments. This study has been supported by the Netherlands Ministry of Economic Affairs, the Ministry of Education, Culture and Science, and the Ministry of Public Housing, Physical Planning and Environment (EET Project "HR-CEL"). The research of W.M.M.K. has been made possible by a fellowship of the Royal Netherlands Academy of Arts and Sciences (KNAW).

[1] D. B. Mitzi, L. L. Kosbar, C. E. Murray, M. Copel, and A. Afzali, Nature (London) **428**, 299 (2004).
[2] S. Koveshnikov, W. Tsai, I. Ok, J. C. Lee, V. Torkanov, M. Yakimov, and S. Oktyabrsky, Appl. Phys. Lett. **88**, 022106 (2006).
[3] H.-S. Kim, I. Ok, M. Zhang, T. Lee, F. Zhu, L. Yu, and J. C. Lee, Appl. Phys. Lett. **89**, 222903 (2006).
[4] B. De Jaeger *et al.*, Microelectron. Eng. **80**, 26 (2005).
[5] M. Taguchi *et al.*, Prog. Photovoltaics **8**, 503 (2000).
[6] N. Jensen, R. M. Hausner, R. B. Bergmann, J. H. Werner, and U. Rau, Prog. Photovoltaics **10**, 1 (2002).
[7] C. J. Först, C. R. Ashman, K. Schwarz, and P. E. Blöch, Nature (London) **427**, 53 (2004).
[8] Y. Yan, M. Page, T. H. Wang, M. M. Al-Jassim, H. M. Branz, and Q. Wang, Appl. Phys. Lett. **88**, 121925 (2006).
[9] R. W. Collins *et al.*, Sol. Energy Mater. Sol. Cells **78**, 143 (2003).
[10] R. W. Collins and B. Y. Yang, J. Vac. Sci. Technol. B **7**, 1155 (1989).
[11] P. J. van den Oever, J. J. H. Gielis, M. C. M. van de Sanden, and W. M. M. Kessels, Thin Solid Films **6**, 92 (2007).
[12] H. Fujiwara, Y. Toyoshima, M. Kondo, and A. Matsuda, Phys. Rev. B **60**, 13598 (1999).
[13] S. de Wolf and G. Beaucarne, Appl. Phys. Lett. **88**, 022104 (2006).
[14] J. S. Christensen, A. G. Ulyashin, K. Maknys, A. Yu. Kuznetsov, and B. G. Svensson, Thin Solid Films **511–512**, 93 (2006).
[15] Y. Cong, I. An, H. V. Nguyen, K. Vedam, R. Messier, and R. W. Collins, Surf. Coat. Technol. **49**, 381 (1991).
[16] H. Fujiwara and M. Kondo, Appl. Phys. Lett. **86**, 032112 (2005).
[17] W. M. M. Kessels, J. P. M. Hoefnagels, E. Langereis, and M. C. M. van de Sanden, Thin Solid Films **501**, 88 (2006).
[18] H. V. Nguyen, Y. Lu, S. Kim, M. Wakagi, and R. W. Collins, Phys. Rev. Lett. **74**, 3880 (1995).
[19] S. Hazra, I. Sakata, M. Yamanaka, and E. Suzuki, Appl. Phys. Lett. **80**, 1159 (2002).
[20] K. H. Jun, K. S. Lim, S. Y. Kim, and S. J. Kim, J. Non-Cryst. Solids **275**, 59 (2000).
[21] Z. H. Lu, D. J. Lockwood, and J.-M. Baribeau, Nature (London) **378**, 258 (1995).
[22] D. J. Lockwood, Z. H. Lu, and J.-M. Baribeau, Phys. Rev. Lett. **76**, 539 (1996).
[23] M. Beaudoin, M. Meunier, and C. J. Arsenault, Phys. Rev. B **47**, 2197 (1993).
[24] A. S. Ferlauto, G. M. Ferreira, J. M. Pearce, C. R. Wronski, R. W. Collins, X. Deng, and G. Ganguly, J. Appl. Phys. **92**, 2424 (2002).
[25] D. C. Marra, E. A. Edelberg, R. L. Naone, and E. S. Aydil, J. Vac. Sci. Technol. A **16**, 3199 (1999).
[26] I. M. P. Aarts, J. J. H. Gielis, M. C. M. van de Sanden, and W. M. M. Kessels, Phys. Rev. B **73**, 045327 (2006).
[27] E. C. Molenbroek, A. H. Mahan, and A. Gallagher, J. Appl. Phys. **82**, 1909 (1997).
[28] D. E. Sweenor, S. K. O'Leary, and B. E. Foutz, Solid State Commun. **110**, 281 (1999).
[29] J. Hale and B. Johs, EASE 2.30, J. A. Woollam Co., Inc., 1999–2004.
[30] H. Arwin and D. E. Aspnes, Thin Solid Films **113**, 101 (1984).
[31] I. An, Y. M. Li, H. V. Nguyen, C. R. Wronski, and R. W. Collins, Appl. Phys. Lett. **59**, 2543 (1991).
[32] In contrast to the original description of the Cody-Lorentz model by Ferlauto and co-workers, here the exponential Urbach tail due to localized states below the band gap is not included, mainly because of the limited

sensitivity to low absorption values and the small spectral range below the band gap.
[33]H. Fujiwara, J. Koh, P. I. Rovira, and R. W. Collins, Phys. Rev. B **61**, 10832 (2000).
[34]A. S. Ferlauto, G. M. Ferreira, J. M. Pearce, C. R. Wronski, R. W. Collins, X. Deng, and G. Ganguly, Thin Solid Films **455**, 388 (2004).
[35]Using the Tauc-Lorentz parametrization, a similar behavior of the band gap as a function of the film thickness was observed.
[36]Note that the height of ε_2 changes despite the constant amplitude parameter A in the CL parametrization [Eq. (2)].
[37]L.-W. Wang and A. Zunger, Phys. Rev. Lett. **73**, 1039 (1994).
[38]G. Cody, C. R. Wronski, B. Abeles, R. B. Stephens, and B. Brooks, Sol. Cells **2**, 227 (1980).
[39]W. Futako, T. Kamiya, C. M. Fortmann, and I. Shimizu, J. Non-Cryst. Solids **266**, 630 (2000).
[40]D. J. Lockwood, Solid State Commun. **92**, 101 (1994).
[41]A. G. Cullis, L. T. Canham, and P. D. J. Calcott, J. Appl. Phys. **82**, 909 (1997).
[42]R. B. Wehrspoon, J.-N. Chazalviel, R. Ozanam, and I. Solomon, Eur. Phys. J.: Appl. Phys. **8**, 179 (1999).
[43]N. F. Mott, Philos. Mag. B **43**, 941 (1981).
[44]N.-M. Park, C.-J. Choi, T.-Y. Seong, and S.-J. Park, Phys. Rev. Lett. **86**, 1355 (2001).
[45]K. Nishio, J. Koga, T. Yamaguchi, and F. Yonezawa, Phys. Rev. B **67**, 195304 (2003).
[46]M. Nishida, Phys. Rev. B **59**, 15789 (1999).
[47]G. Allan, C. Delerue, and M. Lannoo, Phys. Rev. Lett. **78**, 3161 (1997).
[48]G. Allan, C. Delerue, and M. Lannoo, Appl. Phys. Lett. **71**, 1189 (1997).
[49]A. H. M. Smets, W. M. M. Kessels, and M. C. M. van de Sanden, Appl. Phys. Lett. **82**, 1547 (2003).
[50]L. Ley, in *The Physics of Hydrogenated Amorphous Silicon II*, edited by J. D. Hoannopoulos and G. Lucovsky (Springer, Berlin, 1984), Vol. 56, p. 61.
[51]K. Fukutani, M. Kanbe, W. Futako, B. Kaplan, T. Kamiya, C. M. Fortmann, and I. Shimizu, J. Non-Cryst. Solids **227–230**, 63 (1998).
[52]J. P. M. Hoefnagels, Ph.D. thesis, Eindhoven University of Technology.
[53]R. A. Street, *Hydrogenated Amorphous Silicon* (Cambridge University Press, Cambridge, 2005).
[54]It is remarkable that the confinement parameters extracted from the results of Nishida and Lockwood *et al.* show better agreement with the value expected for a *c*-Si film than with the value for an *a*-Si:H film. This might indicate that the ultrathin films show a quasicrystalline structure, as was also suggested by Nishida.